7

Ultra-Wideband Multiwavelength Light Source Utilizing Rare Earth Doped Femtosecond Fiber Oscillator

Nurul Shahrizan Shahabuddin[1],
Marinah Othman[2] and Sulaiman Wadi Harun[1]
[1]Photonics Research Centre, University of Malaya,
[2]Multimedia University,
Malaysia

1. Introduction

Multiwavelength sources are expected to play a major role in future photonic networks, where optical time-division multiplexing (OTDM) and wavelength division multiplexing (WDM) are employed (Teh et al., 2002; Ye et al., 2010; Liu et al., 2006; Parvizi et al., 2011; Harun et al., 2010; Zhong et al., 2010). Various approaches have been taken to develop this source such as by exploiting the nonlinear effects in an optical fiber as well as spectral slicing of a supercontinuum source.

Stimulated Brillouin scattering (SBS) and four wave mixing (FWM) effects are normally used to realize a multiwavelength output whereby the frequency shifts are determined by both the optical fiber structure and pump signal (Chen et al., 2010; Shahi et al., 2009a,2009b; Shahabuddin et al., 2008). A multiwavelength Brillouin fiber laser exhibits wavelength spacing of approximately 0.08 nm depending on the type of material used while FWM frequency shift is known to be dependent on the spacing of the pump signals (Johari et al., 2009; Shahi et al., 2009b; Ahmad et al., 2008). The bandwidth of operation however, is relatively narrow due to the limitation imposed by the erbium doped fiber. Previously, multiwavelength sources also have been demonstrated using superstructure Bragg grating and Fabry perot filter, both have limited range of multiwavelength region and spacing (Teh et al., 2002).

A technique known as spectral slicing can be realized using an arrayed waveguide grating or sagnac loop mirror as the wavelength selective component to slice a broad emission spectrum of amplified spontaneous emission or supercontinuum. It has been shown in many earlier works that slicing of a broadband continuum spectra is capable of generating a multiwavelength laser comb with both spacing tunability and a very wide spectral range (Nan et al., 2004). The supercontinuum light can be produced from a pulsed laser by using the interaction of multiple nonlinear effects such as self-phase modulation (SPM), four-wave mixing (FWM) and stimulated Raman scattering (SRS) in a highly nonlinear optical fiber (Buczynski et al., 2009, 2010; Kurkov et al., 2011; Genty et al., 2004; Lehtonen et al., 2003; Chen et al., 2011; Gu et al., 2010; Akozbek et al., 2006). Spectral slicing allows the channel spacing to be adjusted by changing the length of polarization maintaining fiber (PMF) used in the loop mirror (Ahmad et al., 2009). Hence, spectral slicing provides better spacing tunability as compared to other multiwavelength techniques such as stimulated brillouin scattering as the spacing of the latter highly depends on the waveguide material and structure i.e. the spacing is fixed.

In this chapter, we report a new multiwavelength source using supercontinuum slicing technique. This source use rare earth doped femtosecond fiber oscillator to generate supercontinuum, with multiwavelength operation achieved via spectral slicing of the supercontinuum. Through this technique, the multiwavelength region obtained is the broadest ever to date.

2. Development of mode-locked fiber laser

Mode-locked lasers have found widespread uses in many areas of research, medicine, and industry. The potential of making compact, rugged laser systems with low power consumption at a relatively low cost makes such fiber laser systems very promising candidates for those applications. The stability of the laser is a crucial factor for its applicability. In negative dispersion regime, a soliton pulse is maintained by the interaction of dispersion and nonlinear effect. The bandwidths of both gain fiber and mode-locked filter are neglected (Wise et al., 2008). However, in a normal dispersion fiber laser, the dissipative soliton is maintained by the effects of dispersion, nonlinearity, gain, and spectral filtering (Zhao et al., 2007; Chong et al., 2007). Accordingly, the gain-bandwidth and mode-locked filter play important roles for pulse reshaping and stability (Chong et al., 2007). A stable mode-locked fiber laser can be achieved with the use of polarization maintaining (PM) fibers and a semiconductor saturable-absorber mirror (SESAM) as the mode-locking mechanism. A setup requiring no free-space optics is highly attractive, as it increases stability, and reduces both costs, and the need for maintenance. The fiber mode-locked lasers reported to date obtains mode-locking based on the use of either SESAM or nonlinear polarization rotation (NPR) mechanism (Huan et al., 2006; Harun et al., 2011).

A saturable absorber absorbs the incoming light linearly up to a certain threshold intensity, after which it will saturate and becomes transparent. The recovery time of a semiconductor saturable absorber limits the laser repetition rate. Carbon nanotube (CNT) based saturable absorbers exhibit sub-picosecond recovery times, broadband operation, compatibility with fibers, a small footprint and is simple to fabricate besides being operable in either a transmission or a reflection mode, making them preferable over the more established SESAMs for commercial applications.

Various techniques to achieve stabilized laser sources such as by suppressing the supermode noise, starting the pulse in a laser, and compensating the small distortion caused by the gain fiber, have been reported (Li et al., 1998; Y. Li et al., 2001). In this section, an environmentally stable mode-locked fiber laser based on both NPR and a single wall carbon nanotube saturable absorber (SWCNT-SA) with zero use of free-space optics is demonstrated. The soliton pulse in the cavity can be reshaped and maintained by combining both these mode-locking mechanisms NPR and SWCNT-SA that are based on power-dependent filter. The configuration of our proposed fiber laser is shown in Figure 1. A 10 m long erbium-doped fiber (EDF), which is pumped by a 980-nm laser diode through a 980/1550 nm wavelength division multiplexer (WDM) is used as the gain medium. The EDF has a mode field diameter of 10.4 µm with maximum peak absorption of approximately -10 dB/m at 1550 nm. The group velocity dispersion (GVD) is estimated to be around -42 ps/nm.km at 1550 nm. The other part of the ring cavity uses a 20 m long standard single mode fiber (SMF-28) with a dispersion of 17 ps/nm.km at λ=1545 nm. The net cavity GVD is negative, which enables soliton shaping in the laser. A standard isolator is used to ensure unidirectional operation and to act as a polarizer. A squeezed fiber type polarisation controller (PC) is used to control the polarization states within the cavity. In this experiment, the SWCNT-SA film sandwiched between two FC/PC fiber ferrules to form the fiber-integrated saturable absorber is used for the initiation and stabilization of mode-locking at around 1561 nm region. The SWCNT-SA is fabricated by chemical vapor deposition (CVD) method with an average diameter of 0.8~0.9 nm. The output optical spectrum of the EDFL is monitored by an optical spectrum analyzer (OSA), while the output pulse train and pulse duration are measured using an oscilloscope and an autocorrelator, respectively.

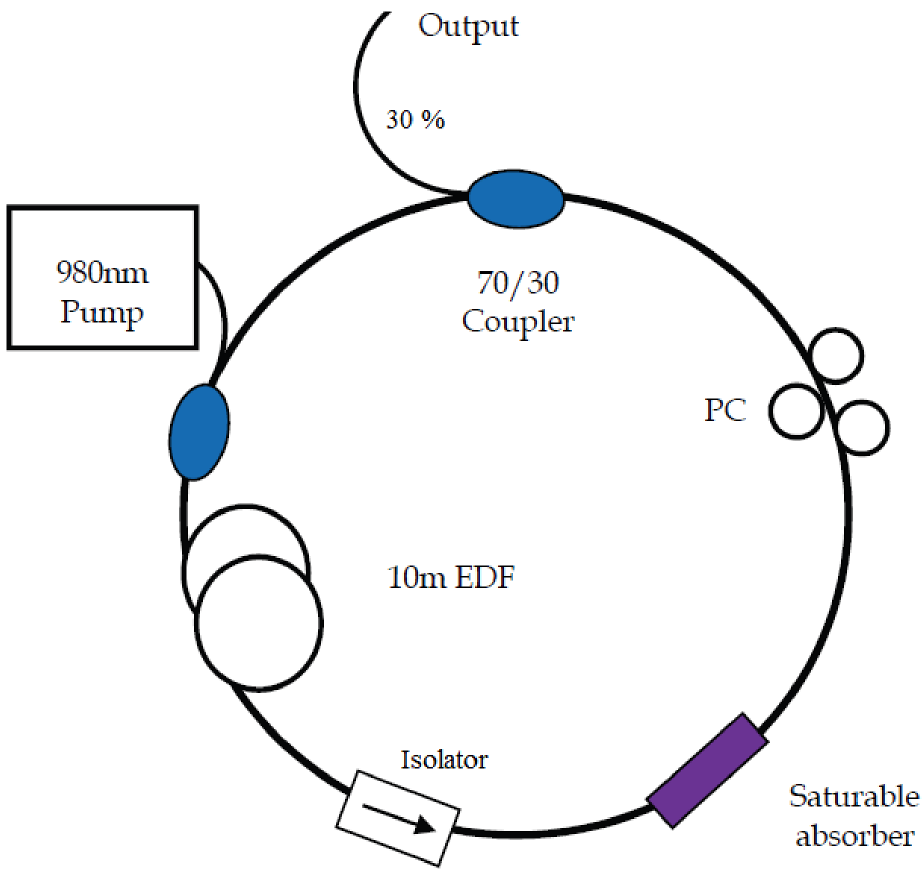

Fig. 1. Experimental setup of the mode-locked fiber laser.

To achieve mode-locking operation, the polarization state of the light within the cavity should be adjusted by using the PC. The pump power threshold for continuous wave laser operation is around 11 mW and a stable self-starting fundamental mode-locked (ML) operation commences at around 140 mW pump power. By altering the polarization state inside the cavity, the optical spectrum can be broadened to initiate Q-switching from which mode-locking operation is obtained. Figure 2 shows the pulse train observed at the output coupler after making both a careful adjustment to the imposed loss accompanied by the variation of the net birefringence of the cavity using a PC. As shown in the figure, a stable fundamental soliton pulse is obtained with a repetition rate of 142 MHz.

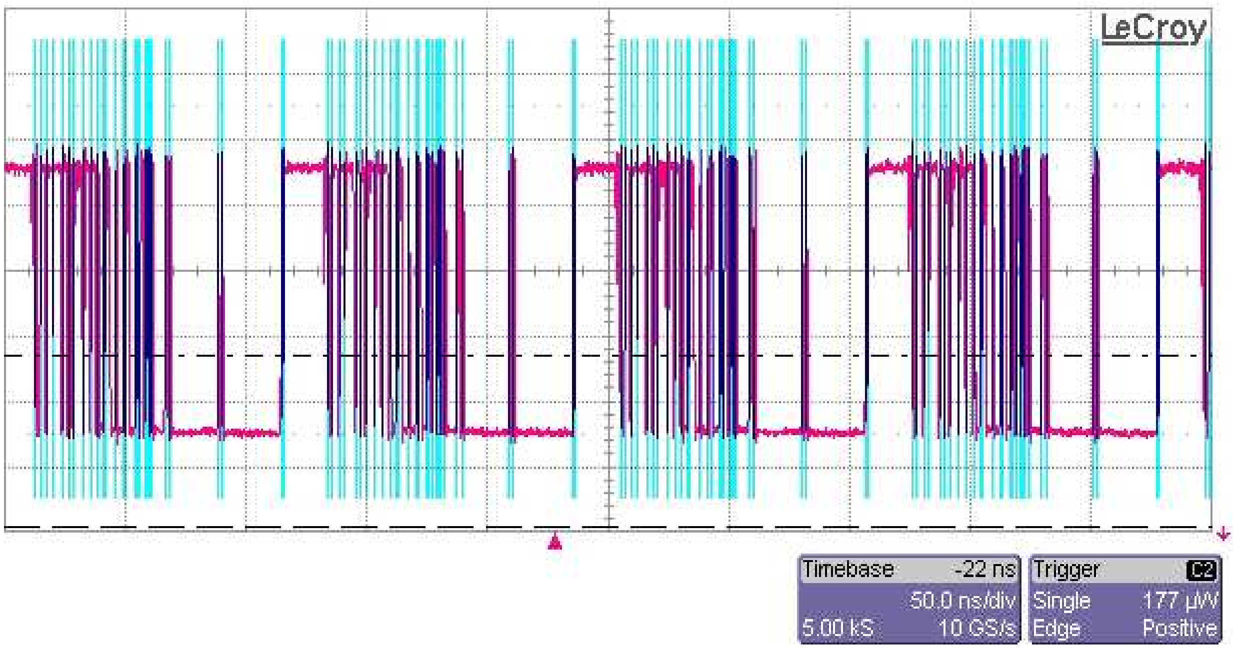

Fig. 2. Pulse train of the proposed soliton EDFL.

The spectral and temporal outputs of the proposed soliton fiber laser are also characterized using an OSA and an autocorrelator. The output spectrum of the mode-locked EDFL obtained from the output port of the coupler is shown in Figure 3. It is clearly seen that the output pulse has a 3 dB bandwidth of 4.5 nm centered at 1558 nm. Kelly sidebands are also evident indicating that the output laser is soliton pulses. These sidebands are a kind of resonant coupling, which for some optical frequencies occur when the relative phase of soliton and dispersive wave changes by an integer multiple of 2π per resonator round trip. The strong Kelly sidebands obtained suggest that the pulse duration is near the minimum possible value. Figure 4 shows an autocorrelation trace of the output pulse from the mode-locked EDFL. The pulse duration is 0.79 ps assuming that the pulse shape follows a $sech^2$ profile. For the purpose of testing the stability of this laser, we kept the laser in the fundamental mode-locked operation and pumped the power at 140 mW without disturbance for a few hours. It was observed that there was no significant change in the spectrum, central wavelength, 3 dB spectrum width and pulse width, output power and repetition rate. This indicates that a stable soliton fiber laser can be achieved using mode-locking based on the combination of both SWNT-SA and NPR.

Passively mode-locked fiber laser can be constructed based on nonlinear polarization rotation without the saturable absorber. This makes a simpler configuration.In this section, a simple mode-locked Bismuth-based Erbium-doped fiber laser (Bi-EDFL) is achieved by using a simple ring cavity structure incorporating a Bismuth-based erbium-doped fiber (EDF), an isolator and a polarisation controller. The short Bi-EDF making up the gain cavity allows the generation of both stable and clean pulses with an increase in the repetition frequency, while its high nonlinearity allows better suppression of the supermode noise. To date, this is the first demonstration of a passively mode-locked fiber laser, which uses such a short length of Bi-EDF together with the nonlinear polarisation rotation (NPR) method.

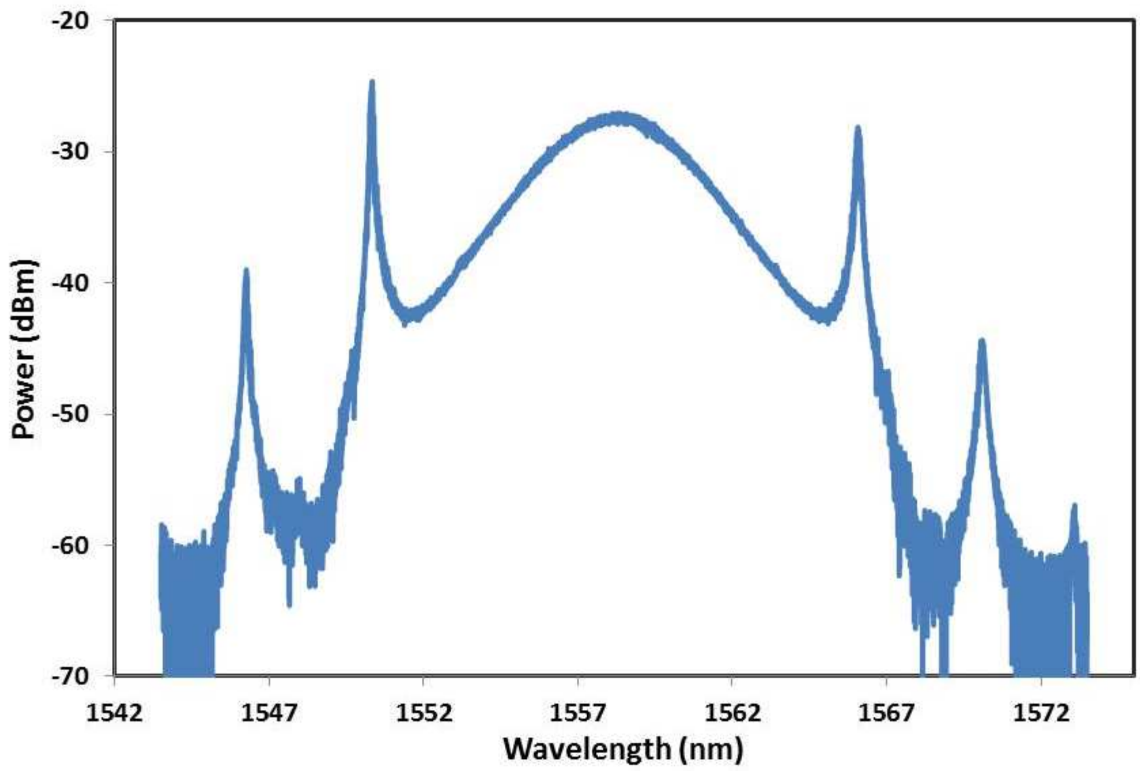

Fig. 3. Optical spectrum of the output of a soliton fiber laser, exhibiting Kelly sidebands.

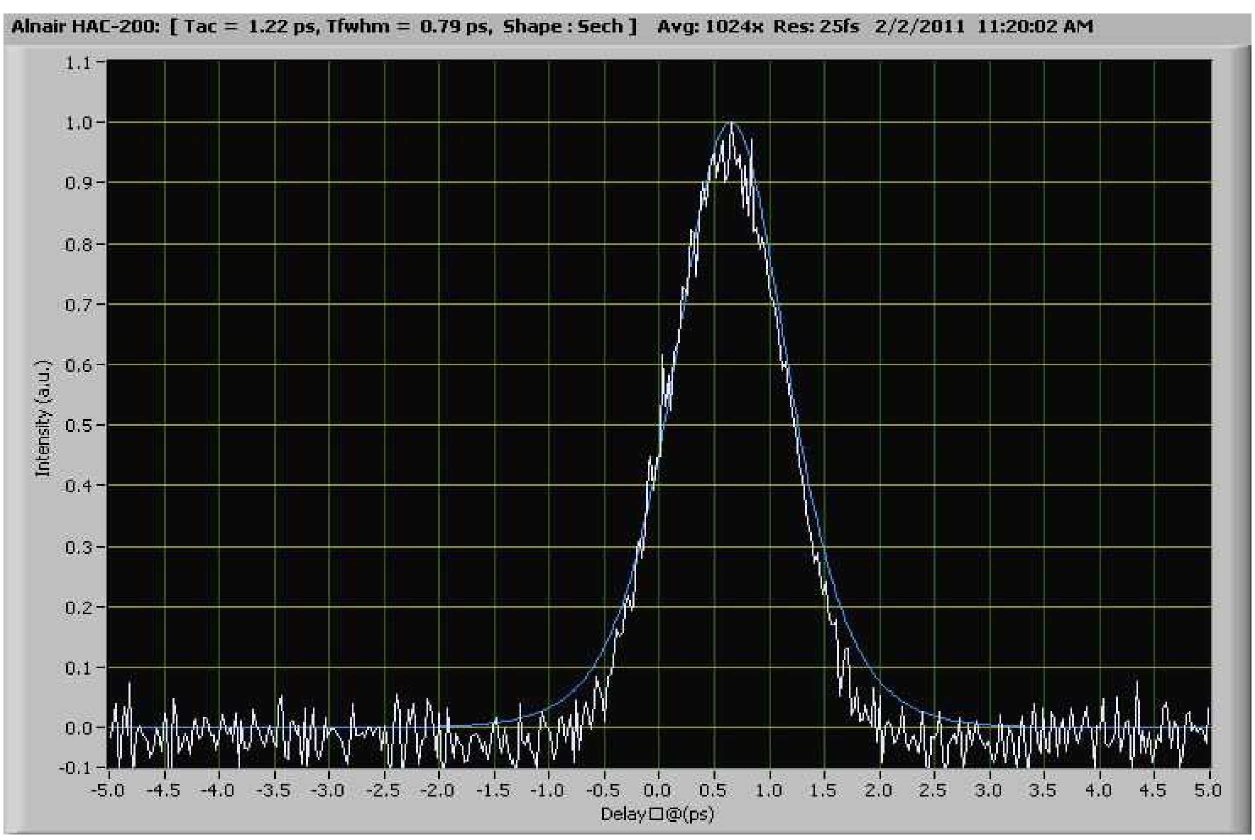

Fig. 4. Autocorrelation trace of the output pulse from the mode-locked EDFL

The experimental set-up of the proposed system for mode-locked Bi-EDFL is illustrated in Figure 5. The Bi-EDFL employs a piece of 49 cm long Bi-EDF, a wavelength division multiplexing (WDM) coupler, an isolator, a polarization controller (PC) and a 3 dB output coupler. The Bi-EDFL cavity consists of a 49 cm long Bi-EDF, and a 2.0 m long SMF-28 which is used in the cavity that is composed of a coupler, polarisation controller, isolator and 980/1550 nm WDM coupler. The Bi-EDF has a nonlinear coefficient of ~60 $(W/km)^{-1}$ at 1550 nm, an Erbium concentration of 3250 ppm, a cut-off wavelength of 1440 nm, a pump absorption rate of 130 dB/m at 1480 nm and a dispersion parameter of 130 ps/km.nm at λ=1550 nm. It is bi-directionally pumped using a 1480 nm laser diode via the WDM to provide an amplification in the C-band region. The other part of the ring cavity uses a standard single mode fiber (SMF-28) with a dispersion of 17 ps/nm.km at λ=1545 nm. A standard polarisation-independent isolator is used to ensure a unidirectional operation and acts as a polarizer. A PC is used to rotate the polarization state and to allow continuous adjustments of the birefringence within the cavity to balance both the gain and loss for the generation of the laser pulses.

A fraction of the stretched laser pulse operating at 1560 nm is extracted through the 50% output of the coupler. The pulse width and repetition rate of the laser pulse are measured to be around 131 fs and 42 MHz, respectively. The output power and spectrum are measured by a power meter and an optical spectrum analyzer (OSA), respectively. The entire experimental setup is fusion-spliced together.

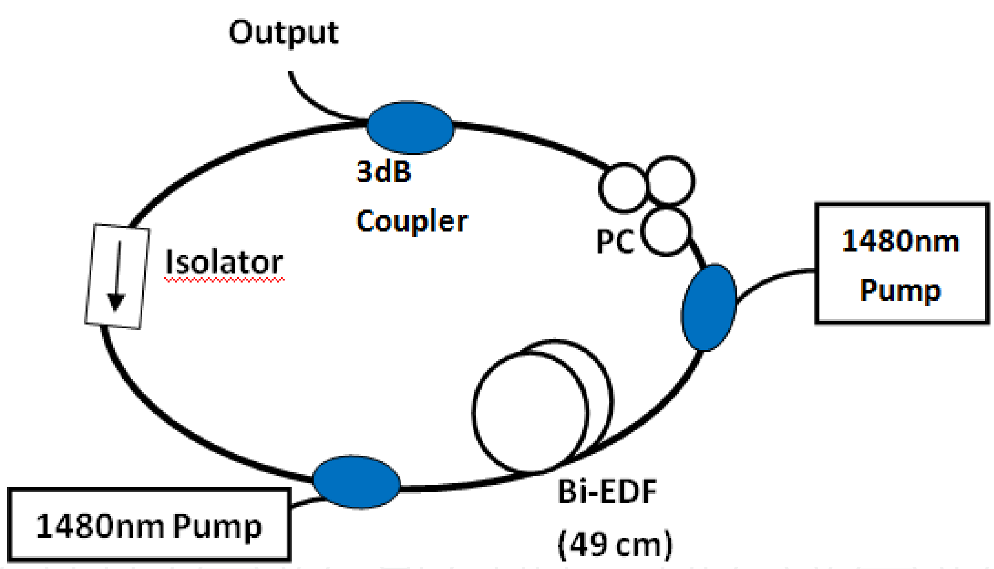

Fig. 5. Experimental set-up for mode-locked fiber laser.

To achieve mode-locking operation, the polarization state of the light within the cavity should be adjusted by using the PC. By altering the polarization state inside the cavity, the optical spectrum can be broadened to initiate Q-switching from which mode-locking operation is obtained. When a linearly polarized light is incident to a piece of weakly birefringent fiber such as a Bi-EDF, the polarization of the light will generally become elliptically polarized in the fiber. The orientation and ellipticity of the resulting polarization of the light is fully determined by the fiber length and its birefringence. However, if the intensity of the light is strong, the nonlinear optical Kerr effect in the fiber must be considered, thus introducing extra changes to the polarization of the light. As the polarization change introduced by the optical Kerr effect depends on the light intensity, if a polarizer or isolator is placed behind the fiber, the transmission of the light through the polarizer will become light intensity dependent. Upon selecting the appropriate orientation of the polarizer, an artificial saturable absorber with an ultra-fast response could then be achieved in such a system, where light of higher intensity experiences less absorption loss on the polarizer. The proposed laser makes use of this artificial saturable absorption to achieve passive mode locking. Once a mode-locked pulse is formed, the nonlinearity of the fiber further shapes the pulse into the ultrashort stretched-pulse.

In the experiment, the 1480 nm pump powers were both fixed at 125 mW. The output spectrum of the mode-locked EDFL obtained after the 3 dB coupler is shown in Figure 6. A broad spectrum with a 3dB bandwidth of 21.7 nm is obtained at the optimum polarization state, which indicates that the output laser has a stretched pulse characteristic. The spectrum has a peak wavelength at 1560 nm. Q-switching operation mode is observed by an oscilloscope in the form of an unstable pulse train with periodic variation in its pulse amplitude. Further adjustment of polarization produces a more stable mode-locked pulse train as shown in Figure 7. The mode-locked pulse train has a constant spacing of 24 ps, which translates to a repetition rate of 42 MHz. The high repetition rate pulse trains are produced from a harmonically mode-locked laser, where multiple pulses circulate within the cavity. The multiple pulses are generated passively in the laser due to the phenomenon known as the soliton energy quantization. The pulse characteristic of the mode-locked EDFL at the 3 dB coupler is also investigated by an autocorrelator. Figure 8 shows the autocorrelator trace of the pulse, which shows the sech^2 pulse profile with a full width half maximum (FWHM) of 131 fs. The output of the femtosecond pulses is also observed to be very stable at room temperature. The operation of the Bi-EDFL can be tuned by incorporating a tunable band-pass filter in the ring cavity. By optimizing the length of the Bi-EDF, a wideband tunable operation is expected to be achieved reaching up to the extended L-band region.

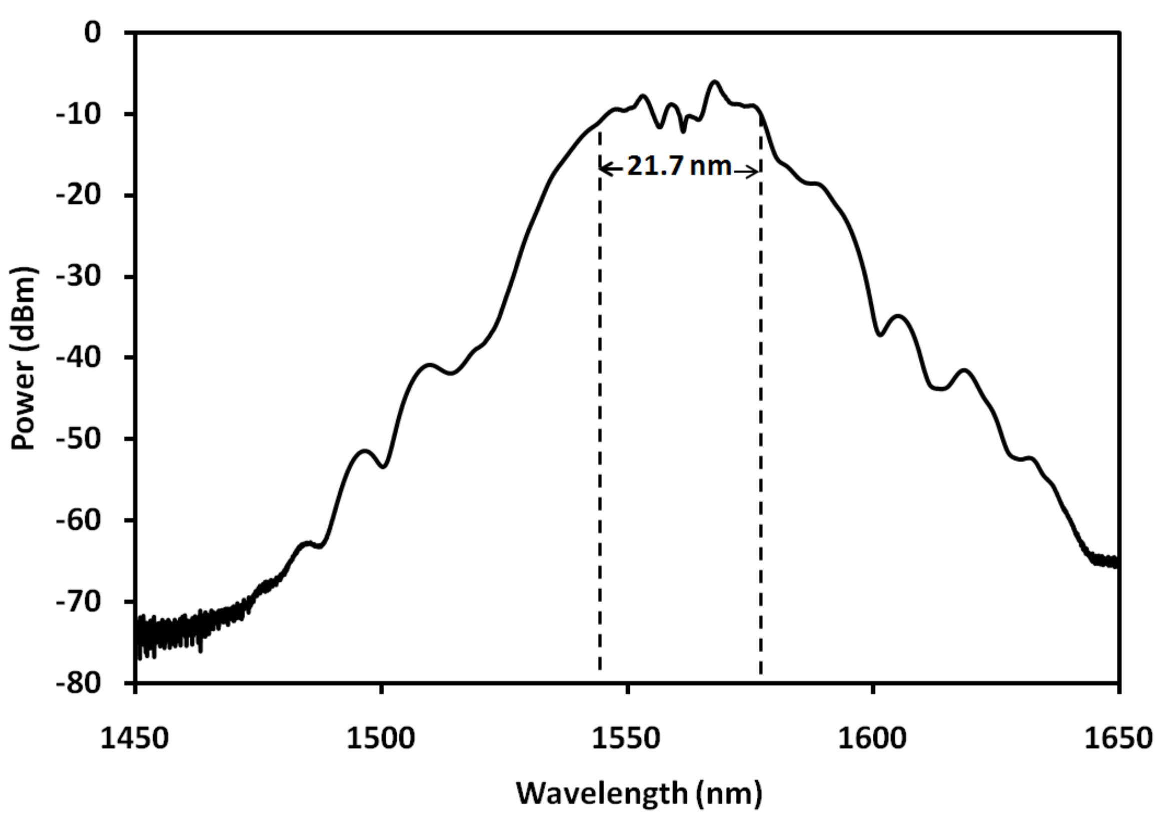

Fig. 6. Optical spectrum of the mode-locked laser.

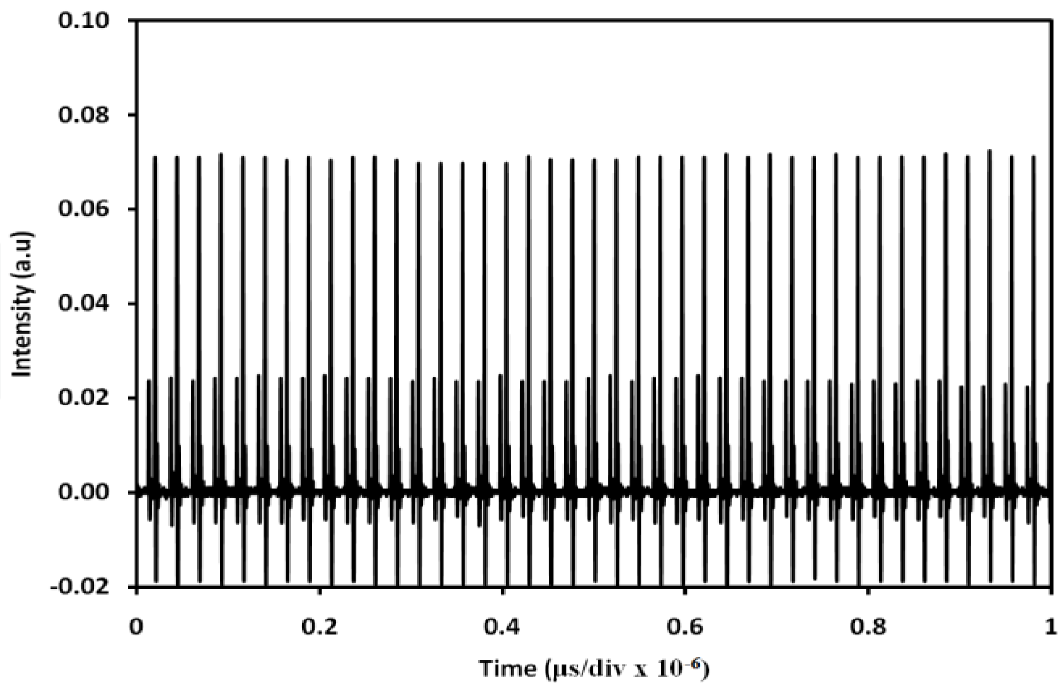

Fig. 7. Pulse train of the passive mode-locked laser with a repetition rate of 42 MHz.

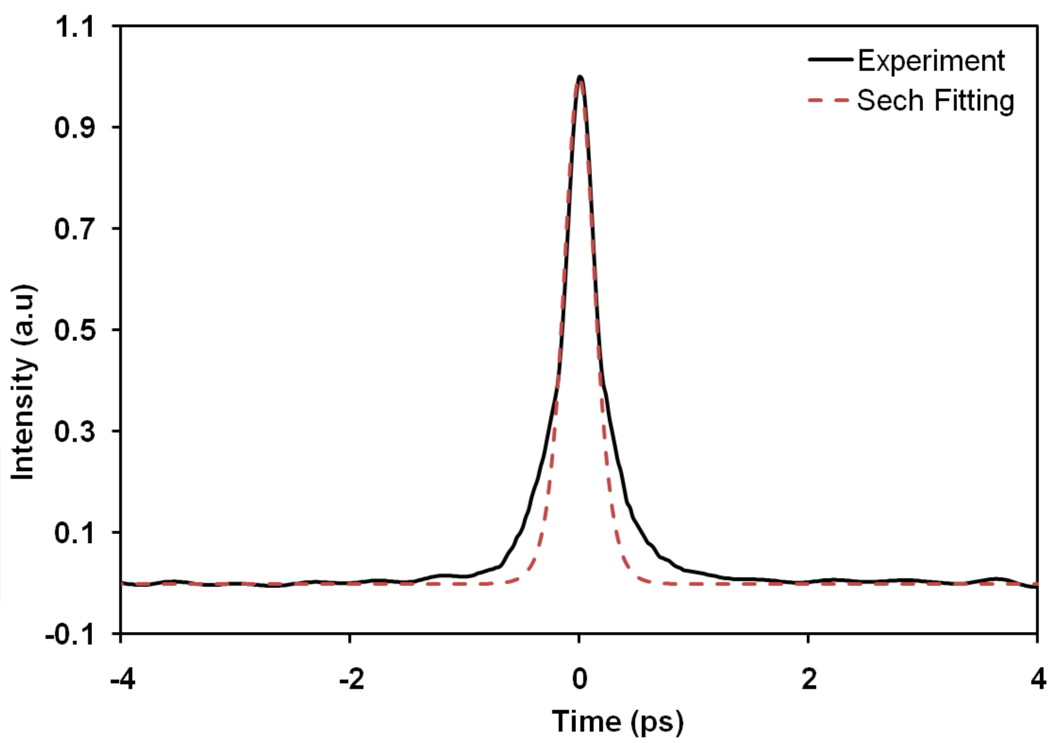

Fig. 8. Autocorrelator pulse trace with FWHM of 131 fs and $Sech^2$ pulse shape.

3. Supercontinuum generation

Supercontinuum generation is the formation of an ultrabroad spectral broadening induced by the coupling of a high peak power sub picosecond pulse laser with a nonlinear optical fiber of adequate length. The supercontinuum spectrum is determined by the sequence of events in the supercontinuum generation, and is dependent on both the pump pulse and the fiber characteristics namely the pump pulse wavelength, power, and pulse duration. The dominant nonlinear effects occurring in the generation of an SC includes self-phase modulation, stimulated Raman scattering and soliton effects. Since supercontinuum was first discovered in 1970 by Alfano (Alfano & Shapiro, 1970), many works have been performed to understand the phenomenon as well as its implementation in practical devices where it has found applications in areas of semiconductor, biology, chemistry, optical coherent tomography, sensing and optical communication, femtosecond carrier-envelope phase stabilization, ultrafast pulse compression, time and frequency metrology, and atmospheric science (Hartl et al., 2001; Kano & Hamaguchi, 2003; Mori, 2003; Alfano, 2006). These included the study of primary events in photosynthesis, nonradiative processes in photoexcited chemicals, excitation of optical phonons, carrier dynamics of semiconductor, frequency clocks and broad spectrum LIDAR.

Specialty fibers such as photonic crystal fibers (PCFs) have high nonlinearity with a managed dispersion profile, and thus, can be used to generate supercontinuum (Parvizi et al., 2010; Russell, 2003). The first supercontinuum generation in a microstructured fiber was reported in 2000 by Ranka et al. Zero dispersion and anomalous dispersion regions could have contributed in higher order soliton generation, pulse compression and ultrabroadband continuum extending from the ultraviolet to the infrared spectral regions. In addition, the pulse broadening in PCF is of great interest for its coherence, brightness and low pulse energy required to generate supercontinuum. The most widely used type of PCF consists of pure silica core surrounded by periodic arrays of air holes, where genuine photonic band-gap guidance can occur. PCFs of this type have attracted much interest because of their potential for lossless and distortion-free transmission, particle trapping, optical sensing, and for novel applications in nonlinear optics (Russell, 2000; Wiederhecker et al., 2007; Benabid et al., 2005).

The supercontinuum can be generated using a picosecond to nanosecond pulses, or even a continuous wave pump where spectral broadening is initiated in the so-called "long pulse" regime (Harun et al., 2011b; Wang et al., 2006; Gorbach et al., 2007). Research is now shifting towards supercontinuum using a more robust and cheaper mode-locked laser, achievable with some innovative designs, as well as the study of the supercontinuum process with picosecond or nanosecond pulsed lasers. As were shown in Figure 1 and Figure 5, we experimentally demonstrated two fiber-based mode-locked lasers using two methods for mode-locking; fiber-based nonlinear polarization rotation (NPR) and saturable absorber. These mode-locked fiber lasers could then be implemented in the experiment to generate supercontinuum.

Figure 9 shows the experimental setup used to generate supercontinuum. A high power amplifier is used to increase the seed pulse peak power to a maximum power of 30 dBm to allow apectral broadening. At the output of the amplifier, the pulse enters a PCF for supercontinuum generation. The supercontinuum spectrum is measured by an optical spectrum analyzer.

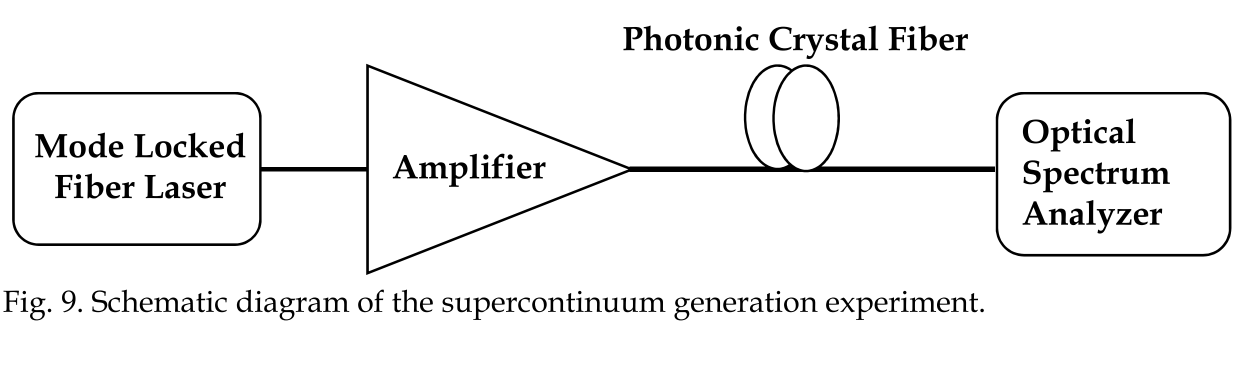

Fig. 9. Schematic diagram of the supercontinuum generation experiment.

Figure 10 shows an SC generation in a 100 m long PCF which is pumped by an amplified 1560 nm mode locked fiber laser at 30 dBm amplified pulse laser power. The mode locked fiber laser used in the experiment has a pulse width of 24 ps with a repetition rate of 42 MHz. The PCF used in the experiment has a zero and -1.5 ps/(km.nm) dispersion at wavelength of 1550 nm and 1580 nm respectively. The PCF length is fixed at the optimised length of 100 m. The nonlinearity coefficient of the PCF is around 11 $W^{-1}km^{-1}$.

As shown in Figure 10, we observe a supercontinuum starting from 600 nm up to 2100 nm at the maximum amplified pulse pump power of 30 dBm. The broad supercontinuum is obtained due to the injection of 1560 nm pulse laser in the anomalous-dispersion regime of the PCF. The pulse initially begins to self-Raman shift to longer wavelengths thus causing asymmetry in the supercontinuum spectrum. When these higher-order solitons break up, parametric four-wave mixing generates frequencies at wavelengths shorter than the zero-dispersion wavelength. With increase in the pump power, there is widening of the spectrum as well as marked improvement of the flatness characteristic.

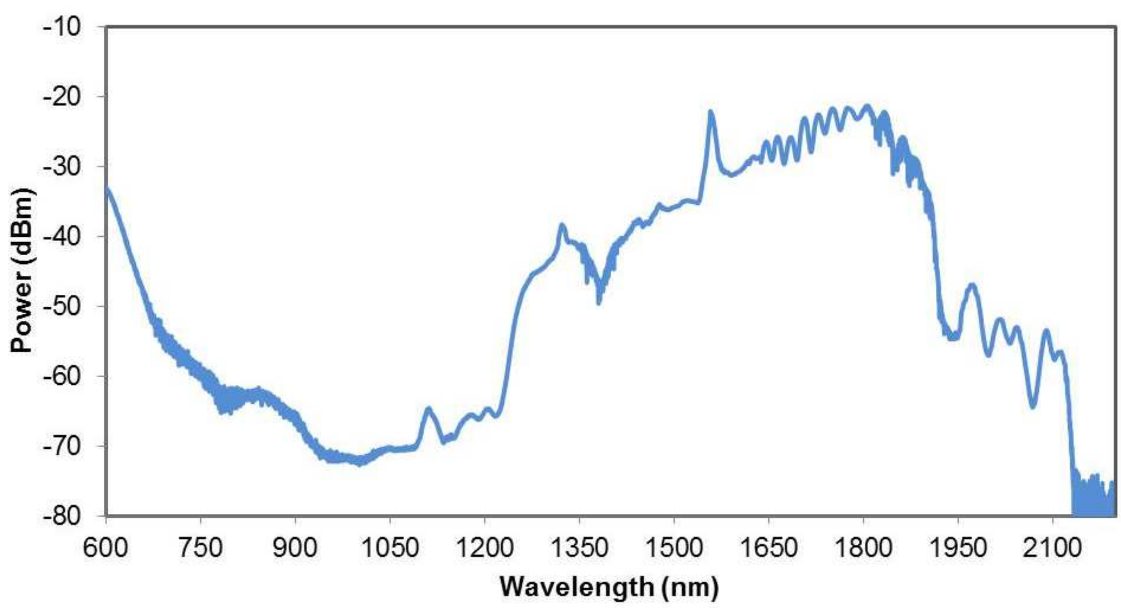

Fig. 10. Supercontinuum generation with 100 m long PCF at fixed average pump power of 30 dBm.

4. Supercontinuum slicing

The supercontinuum generated in the PCF is injected into the loop mirror as shown in Figure 11. In the loop mirror, the supercontinuum source is splitted into two by a 3-dB coupler, where one of the light beams travels in a clockwise direction and the other travels in the opposite direction of the polarization maintaining fiber (PMF). Spectral slicing occurs when the beams interfere constructively and destructively due to the phase differences encountered by the two propagating beams in the loop (Ahmad et al., 2009). Both beams are combined at the end of the fiber coupler to act as a comb filter. Figure 12 shows the multiwavelength spectrum measured by a optical spectrum analyzer through slicing the supercontinuum at pulse pump powers of 30 dBm. The spacing, $\Delta\lambda$ is related to the length, L of the PMF used by the following equation

$$\Delta\lambda = \frac{\lambda}{BL} \quad (1)$$

where B and λ are the birefringence and wavelength, respectively. It is also observed that the comb spectrum is flatter at higher pump power. The spacing of the comb increases as the operating wavelength increases, which agree well with the above equation.

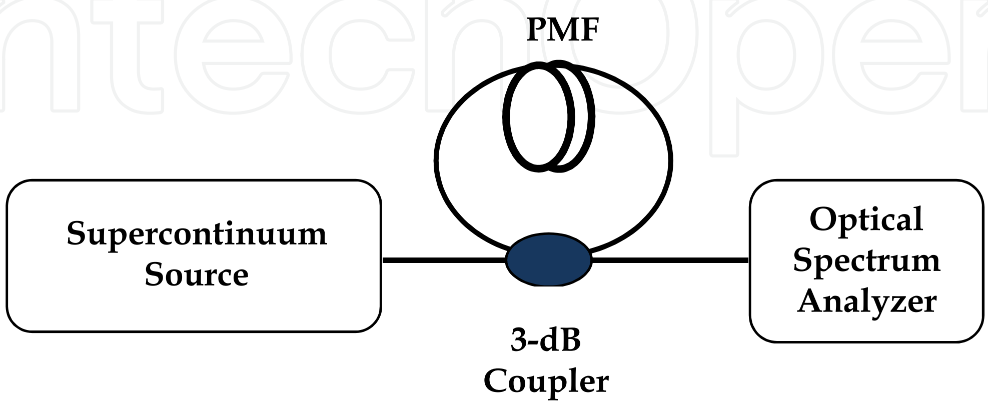

Fig. 11. Loop mirror configuration to slice the supercontinuum source.

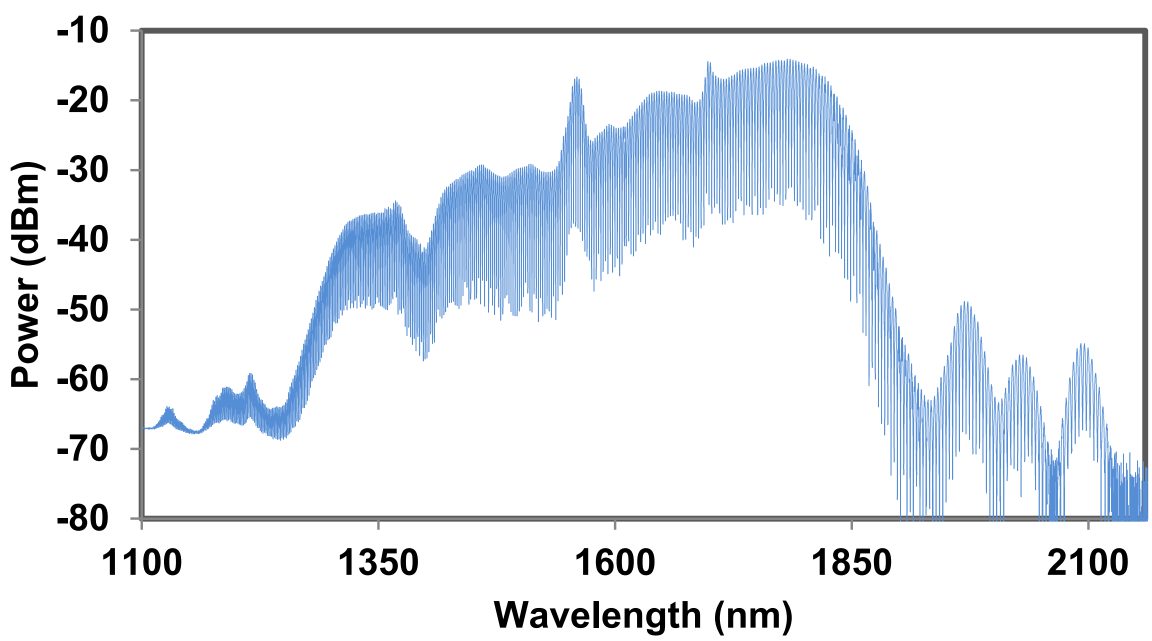

Fig. 12. Multiwavelength comb.

Figure 13 shows the superimposed multiwavelength comb spectrum at different wavelength regions for the supercontinuum with 30 dBm pump pulse power. The multiwavelength comb spectra obtained have an average channel spacings of 2.22 nm and 3.03 nm obtained at 1440 nm and 1750 nm regions, respectively. The spacing of the comb increases as the operating wavelength increases, which agree well with the above equation. In addition, the best signal to noise ratio (SNR) obtained is about 20 dB.

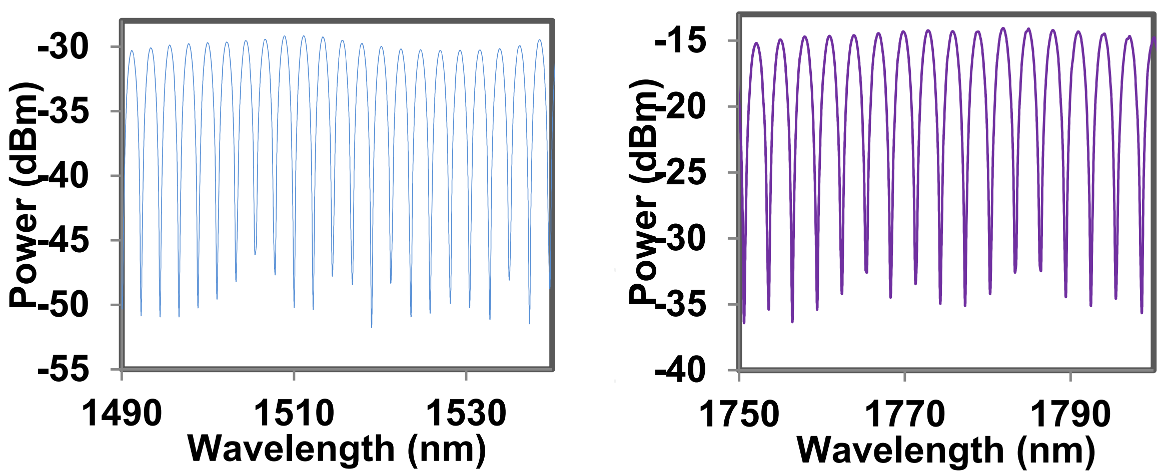

Fig. 13. Sliced spectrum at wavelength regions 1490 nm to 1540 nm and 1750 nm to 1800 nm.

5. References

F. Benabid, F. Couny, J. C. Knight, T. A. Birks and P. S. Russell, "Compact, stable and efficient all-fibre gas cells using hollow-core photonic crystal fibres", *Nature* 434, 488-491 (2005).

X. M. Liu, Y. Chung, A. Lin, W. Zhao, K. Q. Lu, Y. S. Wang and T. Y. Zhang, "Tunable and switchable multi-wavelength erbium-doped fiber laser with highly nonlinear photonic crystal fiber and polarization controllers," *Laser Phys. Lett.* 5, 904–907 (2008).

D. Chen, B. Sun and Y. Wei, "Multi-Wavelength Laser Source Based on Enhanced Four-Wave-Mixing Effect in a Highly Nonlinear Fiber," *Laser Phys*. 20, 1733-1737 (2010).

S. W. Harun, R. Parvizi, N. S. Shahabuddin, Z. Yusoff and H. Ahmad, "Semiconductor optical amplifier-based multi-wavelength ring laser utilizing photonic crystal fiber," *J. Modern Opt*. 57, 637-640 (2010).

M. I. Johari, A. Adamiat, N. S. Shahabuddin, M. N. M. Nasir, Z. Yusoff, H. A. Abdul Rashid, M. H. Al-Mansoori, and P. K. Choudhury, "On the ring cavity multiwavelength Brillouin-erbium fiber laser with partially reflective fiber Bragg grating," *JOSA B* 26(9),1675–1678 (2009).

H. Ahmad, N. S. Shahabuddin, Z. Jusoh, K. Dimyati and S. W. Harun, An enhanced Bismuth-based Brillouin/Erbium fiber laser with linear cavity, *Fiber and Integrated Optics* 27, 35-40 (2008).

N. S. Shahabuddin, S. W. Harun, M. R. Shirazi, and H. Ahmad "A Linear Cavity Brillouin/Bismuth-Based Erbium-Doped Fiber Laser with Enhanced Characteristics", *Laser Physics* 18(11) 1344 (2008).

S. Shahi, S. W. Harun and H. Ahmad, "Multi-wavelength Brillouin fiber laser using Brillouin-Rayleigh scatterings in distributed Raman amplifier," *Laser Phys. Lett*. 6, 737-739 (2009a).

S. Shahi, S. W. Harun, K. S. Lim, A. W. Naji and H. Ahmad, "Enhanced Four-Wave Mixing Efficiency of BI-EDF in a New Ring Configuration for Determination of Nonlinear Parameters ," *Journal of Electromagnetic Waves and Applications* 23, 2397-2407 (2009b)

Y. Nan, C. Lou, J. Wang, T. Wang and L. Huo, "Signal-to-noise ratio improvement of a supercontinuum continuous-wave optical source using a dispersion-imbalanced nonlinear optical loop mirror," *Applied Physics B: Laser and Optics* 76, 61-64 (2004).

R. Buczynski, D. Pysz, T. Martynkien, D. Lorenc, I. Kujawa, T. Nasilowski, F. Berghmans, H. Thienpont, and R.Stepien, "Ultra flat supercontinuum generation in silicate dual core microstructured fiber," *Laser Phys. Lett.* 6(8), 575–581 (2009).

A. S. Kurkov, E. M. Sholokhov and Y. E. Sadovnikova, "All-fiber supercontinuum source in the range of 1550–2400 nm based on telecommunication multimode fiber," *Laser Phys. Lett*. 8, 598-600 (2011).

G. Genty, M. Lehtonen, H. Ludvigsen, and M. Kaivola, "Enhanced bandwidth of supercontinuum generated in microstructured fibers," *Optics Express* 12(15) 3471-3480 (2004).

G. Genty, M. Lehtonen, and H. Ludvigsen "Effect of cross-phase modulation on supercontinuum generated in microstructured fibers with sub-30 fs pulses," *Optics Express* 12, 4614-4624 (2004)

R. Buczynski, H.T. Bookey, D. Pysz, R. Stepien, I. Kujawa, J.E. McCarthy, A.J. Waddie, A.K. Kar, M.R. Taghizadeh, " Supercontinuum generation up to 2.5 um in photonic crystal fiber made of lead-bismuth-galate glass," *Laser Phys. Lett.* 7, 666-672 (2010)

M. Lehtonen, G. Genty and H. Ludvigsen, "Supercontinuum generation in a highly birefringent microstructured fiber," *Applied Physics Letters* 82(14) 2197-2199 (2003)

S. P. Chen, J. H. Wang, H. W. Chen, Z. L. Chen, J. Hou, X. J. Xu, J. B. Chen and Z. J. Liu, "20 W all fiber supercontinuum generation from picosecond MOPA pumped photonic crystal fiber," *Laser Phys*. 21, 519-521 (2011)

Y. Gu, L. Zhan, D. D. Deng, Y. X. Wang and Y. X. Xia, "Supercontinuum generation in short dispersion-shifted fiber by a femtosecond fiber laser," *Laser Phys*. 20, 1459-1462 (2010)

N. Aközbek, S A Trushin, A Baltuˇska, W Fuß, E. Goulielmakis, K. Kosma, F. Krausz, S. Panja, M. Uiberacker, W. E. Schmid, A. Becker, M. Scalora and M. Bloemer, "Extending the supercontinuum spectrum down to 200nm with few-cycle pulses," *New Journal of Physics* 8, 177 (2006).

H. Ahmad, N. S. Shahabuddin and S. W. Harun, "Multi- wavelength source based on SOA and loop mirror," *Optoelectronics and Advanced Materials Rapid Communications* 3(1) 1-3 (2009).

F. W. Wise, A. Chong, and H. William. Renninger, "High-energy femtosecond fiber lasers based on pulse propagation at normal dispersion" *Laser & Photon. Rev*. 2, 58-72, (2008).

L. M. Zhao, D. Y. Tang, H. Zhang,T. H. Cheng,H. Y. Tam,and C. Lu, "Dynamics of gain-guided solitons in all-normal-dispersion fiber laser," *Opt., lett.* 32, 806-1808, (2007).

A. Chong, H. W. Renninger, and F. W. Wise, "Properties of normal-dispersion femtosecond fiber lasers" *J. Opt. Soc. Am. B*, 25, 2140-148, (2008).

A. Chong, H. W. Renninger, and F. W. Wise, "All-normal-dispersion femtosecond fiber laser with pulse energy above 20 nJ," *Opt. lett*. 32, 2408- 2410, (2007).

X. Huan, F. Ga, H. Y. Tama, and P. K. A. Wai, "Stable and uniform multiwavelength erbium doped fiber laser using nonlinear polarization rotation," *Optics express*, 14, 8205-8210(2006).

S. W. Harun, R. Akbari, H. Arof and H. Ahmad, "Mode-locked bismuth-based erbium-doped fiber laser with stable and clean femtosecond pulses output," *Laser Phys.* Lett. 8, pp. 449-452 (2011).

Y. Li, C. Lou, J. Wu, B. Wu, and Y. Gao, "Novel method to simultaneously compress pulses and suppress supermode noise in actively mode-locked fiber ring laser," *IEEE Photon. Technol. Lett*., 10, 1250-1252 (1998).

Z. Li, C. Lou, K. T. Chan, Y. Li, and Y. Gao, "Theoretical and experimental study of pulse-amplitude-equalization in a rational harmonic mode-locked fiber ring laser," *IEEE J. Quantum Electron.*, 37, 33-37 (2001).

R. R. Alfano and S. L. Shapiro, "Emission in region 4000 to 7000 a via 4- photon coupling in glass," *Physical Review Letters* 24(11), 584 (1970).

I. Hartl, X. D. Li, C. Chudoba, R. K. Ghanta, T. H. Ko, J. G. Fujimoto, J. K. Ranka, and R. S. Windeler, "Ultrahigh-resolution optical coherence tomography using continuum generation in an air-silica microstructure optical fiber," *Opt. Lett*. 26, 608-610 (2001)

H. Kano and H. Hamaguchi, "Characterization of a supercontinuum generated from a photonic crystal fiber and its application to coherent Raman spectroscopy," *Opt. Lett.*, 28, 2360-2362 (2003).

K. Mori, K. Sato, H. Takara, and T. Ohara, Supercontinuum lightwave source generating 50 GHz spaced optical ITU grid seamlessly over S-, C- and L-bands," *Electron. Lett*. 39, 544-546, (2003).

R. R. Alfano, (2nd) 2006. *The Supercontinuum Laser Source: Fundamentals and Updated References*, Springer, ISBN 0-387-24504-9, New York

R. Parvizi, S. W. Harun, N. S. Shahbuddin, Z. Yusoff and H. Ahmad, "Multi-wavelength bismuth-based erbium-doped fiber laser based on four-wave mixing effect in photonic crystal fiber, *Optics and Laser Technol*. 44, 1250-1252 (2010).

P. Russell, Photonic crystal fibers, *Science* 299, 358–62 (2003)

J. K. Ranka, R. S. Windeler, and A. J. Stentz, Visible continuum generation in air-silica microstructure optical fibers with anomalous dispersion at 800 nm, *Opt. Lett*. 25, 25–27 (2000)

G. S. Wiederhecker, C. M. B.Cordeiro, F.Couny, F. Benabid, S. A. Maier, J. C. Knight, C. H. B. Cruz and H. L.Fragnito, "Field enhancement within an optical fibre with a subwavelength air core,*Nature Photonics* 1, 115-118 (2007).

S. W. Harun, R. Akbari, H. Arof and H. Ahmad, "Supercontinuum generation in photonic crystal fiber using femtosecond pulses," *Laser Phys*. 21, 1215-1218 (2011).

A. V. Gorbach & D.V. Skryabin, "Light trapping in gravity-like potentials and expansion of supercontinuum spectra in photonic-crystal fibres," *Nat. Photonics* 1, 653-657 (2007).

A. Martinez and S. Yamashita, "Carbon Nanotube-Based Photonic Devices: Applications in Nonlinear Optics, In: *Carbon Nanotubes in Electron Devices,* Jose Mauricio Marulanda, pp. 367-386, Intech, Retrieved from http://www.intechopen.com/download/pdf/pdfs_id/17299

R. Parvizi, S. W. Harun, N. M. Ali, N. S. Shahabuddin and H. Ahmad, " Photonic crystal fiber-based multi-wavelength Brillouin fiber laser with dual-pass amplification configuration," *Chinese Optics Lett*. 9, 021403 (2011).

Z. Wang, C. Y. Wang, Y. K. Han, S. Y. Cao, Z. G. Zhang and L. Lai, "Octave-spanning spectrum generation in Ti : sapphire oscillator," *Opt. & Laser Technol*. 38, 641-644 (2006).

W. Ye, W. Liu, T. Chen, D. Z. Yang and Y. H. Shen, "Erbium-ytterbium co-doped multi-wavelength double-clad fiber laser around 1612 nm," *Laser Phys.* 20, 1636-1640 (2010).

K. Zhong, J. S. Li, D. G. Xu, X. Ding, R. Zhou, W. Q. Wen, Z. Y. Li, X. Y. Xu, P. Wang and J. Q. Yao, "Multi-wavelength generation based on cascaded Raman scattering and self-frequency-doubling in KTA," *Laser Phys.* 20, 750-755 (2010).

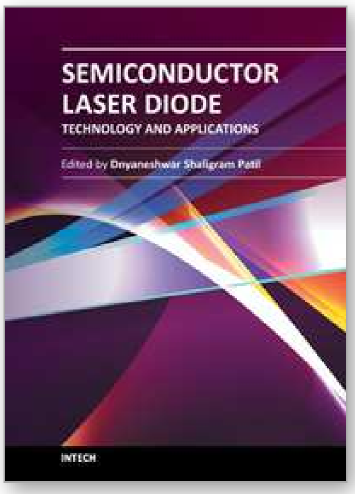

Semiconductor Laser Diode Technology and Applications

Edited by Dr. Dnyaneshwar Shaligram Patil

ISBN 978-953-51-0549-7

Hard cover, 376 pages

Publisher InTech

Published online 25, April, 2012

Published in print edition April, 2012

This book represents a unique collection of the latest developments in the rapidly developing world of semiconductor laser diode technology and applications. An international group of distinguished contributors have covered particular aspects and the book includes optimization of semiconductor laser diode parameters for fascinating applications. This collection of chapters will be of considerable interest to engineers, scientists, technologists and physicists working in research and development in the field of semiconductor laser diode, as well as to young researchers who are at the beginning of their career.

InTech Europe
University Campus STeP Ri
Slavka Krautzeka 83/A
51000 Rijeka, Croatia
Phone: +385 (51) 770 447
Fax: +385 (51) 686 166
www.intechopen.com

InTech China
Unit 405, Office Block, Hotel Equatorial Shanghai
No.65, Yan An Road (West), Shanghai, 200040, China
中国上海市延安西路65号上海国际贵都大饭店办公楼405单元
Phone: +86-21-62489820
Fax: +86-21-62489821